



Non-parallel vortex instability of natural convection flow over a non-isothermal inclined flat plate with simultaneous thermal and mass diffusion

M Acharya^{*1}, L.P Singh² and G.C Dash³

¹ Department of Physics, College of Basic Sciences and Humanities, Orissa University of Agriculture and Technology, Bhubaneswar-751 003, Orissa, India

² Department of Physics, Utkal University, Bhubaneswar-751 004, Orissa, India

³ Koushtuv Institute of Self Domain, Bhubaneswar-751 024, Orissa, India

E-mail: manastaranjan_acharya@yahoo.co.in

Received 30 March 2006, accepted 27 June 2006

An analysis is performed to study the heat mass transfer and non-parallel vortex instability characteristics of buoyancy induced flows from simultaneous diffusion of heat and mass on laminar boundary layers adjacent to horizontal and inclined surfaces with variable surface temperature $T_w(x) = T_\infty + Ax^n$ where n is a constant to be taken as 0, 1/3 or 1. Numerical results are obtained for a Prandtl number of 0.7 over a range of buoyancy numbers and various angles of inclination from the horizontal ϕ . The preparation of solution algorithm with the recursion formulae tedious for system of first order equations to be solved with block elimination method. Therefore, matrix-solver algorithm [26] is used to carry out operations required in the block elimination method. For a given angle ϕ , it is found that when the two buoyancy forces from thermal and mass diffusion act in the same direction, both the surface heat and mass transfer rates increase causing the flow to become more susceptible to the onset of instability. However, the fluid flow becomes stable when the two buoyancy forces act in the opposite directions. On the other hand, as opposed the heat and mass transfer rates are enhanced but instability of the flow to the vortex mode of disturbance decreases and eventually at $\phi = 90^\circ$ deg. Results from the present non-parallel flow analysis are compared with the available experimental data. It is observed that calculation is close to experimental data.

Keywords: Vortex instability, non-parallel flow, buoyancy ratio parameter, thermal and mass diffusion

AMS Nos: 47-20 Bp, 47-11 -f, 47-15 Fe

Introduction

Natural convection widely exists in energy and chemical industry and convective flow over heated surface, the effect of buoyancy force may play an important role in the transport of mass. If there exists a concentration gradient in the fluid in addition to temperature gradient, the buoyancy force due to mass diffusion is also significant. Thus, buoyancy forces are induced simultaneously by thermal diffusion and mass diffusion of species concentration in a transport process. Representative fields of interest using buoyancy effects include flow from simultaneous thermal and mass diffusion include flow from chemical processing equipment, formation and dispersion of fog, distribution of temperature and moisture over agricultural fields and groups of fruit trees, damage of crops

due to freezing and pollution of environment. The problems of combined effects of thermal and mass diffusion in natural convection flow have been studied for vertical and horizontal flat plate [1,2]. Chen and Yuh [3] have generalised the analysis to flow over an inclined plate in which they have neglected the streamwise pressure gradient term in the momentum equation and obtained similarity solutions for the flow, thermal and concentration fields. In a large number of technical applications, the surface heating conditions are non-uniform and induced buoyant flow is laminar. This is why the natural convection with non-uniform surface heating has received considerable attention [4].

Two types of instabilities are known to occur in the boundary layer induced by buoyancy force. One of which is a stationary mode and the other is a travelling mode instability. Only the

*Corresponding Author

stationary mode instability is considered. The instability of vertical inclined and horizontal natural convection flows has also been analysed extensively by many investigators [5-14]. The buoyancy induced flows and their stability characteristics have been studied by Gebhart [15]. Some of the previous studies have treated the wave mode of instability, while the others have analysed vortex mode of instability. However, the majority of these studies except for [9] and [12], have considered the flow situation in which the buoyancy force is induced solely by the temperature variations in the fluid. The wave instability of natural convection flows with combined buoyancy modes of thermal and mass diffusion has been investigated by Pera and Gebhart [9] for a horizontal plate with both Prandtl number and Schmidt number equal to 0.7 and by Boura and Gebhart [12] for a vertical plate with a Prandtl numbers of 0.7 and Schmidt numbers of 0.2, 0.94 and 2.0. The vortex instability of natural convection flows under the combined thermal and mass diffusion process, has been analysed by Chen *et al* [17]. Mixed mode convection in an inclined slot has been studied by Fujimora and Kelly [18].

In contrast to theoretical studies, the experimental work on the instability of inclined natural convection flows has been confined to situations in which there is no mass diffusion [19-21]. From the experimental work of Lloyd and Sparrow [16] on natural convection flow in water over inclined heated plates, it has been concluded that for inclination angles larger than 17 deg (relative to the vertical), the instability is characterised by Tollmien-Schlichting - the longitudinal vortex mode, whereas for inclination angle less than 14 deg, the instability is characterised by wave mode. In the range between 14 deg and 17 deg, the two modes of instability were found to coexist.

In all the analytical studies [5-7, 10, 13, 22] on the vortex mode of instability of laminar flow over inclined heated plates, a linear parallel flow model is employed in which the amplitude functions of disturbances are assumed to be independent of the streamwise coordinate. The parallel flow analysis has provided critical Grashof numbers that are two to three order magnitude lower than those of experimental values. However, studies on vortex instability of natural convection flow over horizontal flat plate [14] and vortex instability of forced convection flow [23-25] predicted that non-parallel flow analysis yields more realistic predictions of the instability characteristics, when compared with experimental data than the parallel flow analysis. In non-parallel flow analysis, the main flow and thermal fields (or concentration fields) are treated as non-parallel. Due to the fact that analytical results of instability of flow depend on the accuracy of main flow solution, an analysis of vortex instability of natural convection flow over horizontal and inclined surface should be preceded with an accurate and complete solution of main flow. Such a main flow solution under the simultaneous effect of thermal and mass diffusion with the variable surface temperature, has not been studied and this constitutes the first part of present investigation.

In the present study, the non-parallel vortex instabilities of horizontal and inclined natural convection flows from simultaneous thermal and mass diffusion is analysed by employing the non-parallel flow model in which the streamwise variations of disturbances are taken. The surface temperature of the plate is treated as non-uniform and varies as $T_w(x) = T_\infty + Ax^n$. The governing conservation equations in the laminar boundary layer are transformed into a system of dimensionless equations such that the non-similarity parameter $\xi(x)$ varies with x to a positive power and depends also on angle of inclination from the horizontal ϕ . This system of equations for the main flow, thermal and concentration fields with boundary conditions, is solved by block elimination method described by Cebeci and Cousteix [26]. As the number of order equations to be solved with the block elimination method is 9, the preparation of solution algorithm with the required formula becomes tedious. So we use matrix - solver algorithm described by Cebeci and Cousteix [26].

The stability analysis is based on linear non-parallel flow [27, 28]. The disturbance quantities are assumed to be of form of a stationary vortex roll, and have been found to remain unchanged with time and periodic in the spanwise direction. The disturbance quantities are assumed to be a function of (x, y, z) , independent of time t . This disturbance quantity is superimposed on the steady two-dimensional main flow quantities. The resulting partial differential equations for disturbance amplitude functions along with the boundary conditions are converted into an eigen value problem which is solved numerically by finite difference method [29] in conjunction with Muller shooting procedure.

2. Mathematical formulation

2.1 The main flow, thermal and concentration fields

We consider an inclined flat plate, which makes an acute angle ϕ from the horizontal with its heated surface facing up and an otherwise quiescent fluid at temperature T_∞ and concentration C_∞ . The physical coordinates are chosen such that x is measured from the leading edge of the plate and measured normal to the plate. The surface temperature of plate varies as $T_w(x) - T_\infty = Ax^n$, where A and exponent n are real constants. The following assumptions are made:

- (i) The fluid properties are assumed to be constant except for the body force terms in the momentum equations which are approximated by the Boussinesq relations.
- (ii) Fluid flows with low concentration level are considered such that the diffusion thermo and the diffusion effect, as well as the interfacial velocity due to mass diffusion, are neglected.

- (iii) Viscous dissipation in the energy equation is neglected
- (iv) No chemical reactions are taking place in the flow
- (v) The boundary layer equations for mass, momentum, energy and species concentration are applicable

Based on these assumptions, the governing conservation equations of the laminar boundary layer flow can be written as

$$\rho \frac{\partial U}{\partial x} + \rho \frac{\partial V}{\partial y} = 0, \quad (1)$$

$$\rho \frac{\partial U}{\partial x} + \rho \frac{\partial V}{\partial y} = g \beta \cos \phi \frac{\partial T}{\partial x} \int_0^{\infty} (T - T_{\infty}) dy + g \beta^* \cos \phi \frac{\partial C}{\partial x} \int_0^{\infty} (C - C_{\infty}) dy + g \beta \sin \phi (T - T_{\infty}), \quad (2)$$

$$\rho \frac{\partial T}{\partial x} + \rho \frac{\partial T}{\partial y} = K \frac{\partial^2 T}{\partial y^2}, \quad (3)$$

$$\rho \frac{\partial C}{\partial x} + \rho \frac{\partial C}{\partial y} = D \frac{\partial^2 C}{\partial y^2}, \quad (4)$$

where all the terms are defined in the nomenclature section. The first two terms on the right-hand side of eq. (2) represent the transverse pressure gradient induced by the normal component of the buoyancy forces, respectively from the temperature and concentration variations in the fluid and third and fourth terms represent the axial component of the respective buoyancy forces. The boundary conditions for equations (1-4) are

$$\begin{aligned} U = 0, \quad V = v_w, \quad T = T_w(x) = T_{\infty} + A x^n, \\ (C - C_{\infty})(x) = C_{\infty} + B x^n \text{ at } y = 0; \\ U \rightarrow 0, \quad T \rightarrow T_{\infty}, \quad C \rightarrow C_{\infty}, \quad \text{as } y \rightarrow \infty \end{aligned} \quad (5)$$

Eq. (2) reduces to that for a vertical plate [1] when $\phi = \pi/2$, and to that of horizontal plate, when $\phi = 0$ deg. Eqs. (1-5) can be transformed into dimensionless equation by employing the dimensionless coordinate $\xi(x)$ and $\eta(x, y)$ [13]

$$\xi = \left(\frac{Gr_{x,i} \cos \phi}{5} \right)^{1/5} \tan \phi, \quad \eta = \frac{y}{x} \left(\frac{Gr_{x,i} \cos \phi}{5} \right)^{1/5} \quad (6)$$

Along with the reduced stream function $\phi(\xi, \eta)$, the dimensionless temperature $\theta(\xi, \eta)$ and dimensionless mass fraction $\lambda(\xi, \eta)$ defined respectively by,

$$\psi(x, y) = 5 f(\xi, \eta) \nu \left(\frac{Gr_{x,i} \cos \phi}{5} \right)^{1/5}$$

$$\theta(\xi, \eta) = T - T_{\infty} / (T_w(x) - T_{\infty}),$$

$$\lambda(\xi, \eta) = C - C_{\infty} / (C_w(x) - C_{\infty}) \quad (7)$$

The non-similar parameter $\xi(x)$ measured the combined effects of buoyancy force $Gr_{x,i}$ and inclination angle ϕ on the flow and heat transfer characteristics. $\psi(x, y)$ is stream function that satisfies continuity eq. (1) with $U = \partial \psi / \partial y$ and $V = -\partial \psi / \partial x$. $Gr_{x,i}$ is the local Grashof number defined by

$$Gr_{x,i} = g \beta (T_w(x) - T_{\infty}) x^3 / \nu^2 \quad \text{and} \quad T_w(x) - T_{\infty} = A x^n.$$

$n = 0$ corresponds to uniform wall temperature (UWT).

Using above transformation, the system of equations reduces to the following form

$$\begin{aligned} f''' + (n+3)ff' - (2n+1)(f')^2 + \xi(\theta + N\lambda) \\ + \frac{1}{5}(2-n)\eta(\theta + \lambda N) + \frac{1}{5}(4n+2) \int_0^{\infty} (\theta + \lambda N) d\eta \\ + \frac{1}{5}(n+3)\xi \int_0^{\infty} \left(\frac{\partial \theta}{\partial \xi} + N \frac{\partial \lambda}{\partial \xi} \right) d\eta \\ = (n+3)\xi \left[f' \frac{\partial f'}{\partial \xi} - f'' \frac{\partial f}{\partial \xi} \right], \end{aligned} \quad (8)$$

$$\begin{aligned} \theta'' + (n+3)Pr(f\theta' - 5nPr'f\theta) \\ = (n+3)Pr\xi \left[f' \frac{\partial \theta}{\partial \xi} - \theta' \frac{\partial f}{\partial \xi} \right], \end{aligned} \quad (9)$$

$$\begin{aligned} \lambda'' + (n+3)Sc(f\lambda' - 5nScf\lambda) \\ = (n+3)Sc\xi \left[f' \frac{\partial \lambda}{\partial \xi} - \lambda' \frac{\partial f}{\partial \xi} \right], \end{aligned} \quad (10)$$

$$f'(\xi, 0) = f(\xi, 0) = 0, \quad f(\xi, 0) + \xi \frac{\partial f(\xi, 0)}{\partial \xi} = 0$$

$$\theta(\xi, 0) = 1, \quad \lambda(\xi, 0) = 1,$$

$$f'(\xi, \infty) = \theta(\xi, \infty) = \lambda(\xi, \infty) = 0. \quad (11)$$

The primes indicate partial differentiation with respect to η and N is the buoyancy ratio parameter defined as

$$\begin{aligned} N = \left(\beta^* (C_w(x) - C_{\infty}) \right) / \left(\beta (T_w(x) - T_{\infty}) \right) \\ = Gr_{x,i} / Gr_{x,i} \end{aligned} \quad (12)$$

with $Gr_{x,i} = g \beta^* (C_w(x) - C_{\infty}) x^3 / \nu^2$ is the local Grashof number for mass diffusion. The buoyancy ratio parameter N measures the relative importance of buoyancy force between mass and thermal diffusion that drives the flow. There is no mass diffusion when $N = 0$, the buoyancy forces from mass and

thermal diffusion act in the same direction when $N > 0$ and $N < 0$ indicates both the forces act in opposite directions. The non-similar parameter $\xi(x)$ is a measure of plate inclination ϕ as well as thermal buoyancy force intensity $f(\xi, 0) = 0$ indicates the normal velocity v_w at the wall, associated with the species diffusion process, is negligibly small. This assumption is valid when the condition

$$v_w \sqrt{\nu} \ll \beta \left((Gr_{L,t} \cos \phi) / 5 \right)^{1/5} \quad (13)$$

or using Fick's law,

$$\frac{1}{3} S_L [C_w(x) - C_\infty] [-\lambda'(\xi, 0)] \ll 1 \quad (14)$$

is satisfied

The physical quantities of interest include local Nusselt number N_{ax} , local Sherwood number Sh_L (local chemical species transfer ratio), the local wall shear stress τ_w and axial velocity distribution. In terms of dimensionless variables, these quantities can be expressed as

$$Sh_L \left((Gr_{L,t} \cos \phi) / 5 \right)^{-1/5} = -\lambda'(\xi, 0), \quad (15)$$

$$Nu_L \left((Gr_{L,t} \cos \phi) / 5 \right)^{-1/5} = -\theta'(\xi, 0), \quad (16)$$

$$\tau_w \left(x^{2/5} / 5 \mu \nu \right) \left((Gr_{L,t} \cos \phi) / 5 \right)^{-1/5} = f''(\xi, 0) \quad (17)$$

2.2 Formulation of stability problem

The linear non-parallel flow stability theory is considered in the present analysis. It is found from the experiment that the longitudinal vortex rolls remain unchanged with time and periodic in the spanwise direction z . Thus, the disturbance quantities for velocity components u' , v' , w' , pressure p' , temperature t' and species concentration c' are assumed to be functions of (x, y, z) and independent of time. These disturbance quantities are superimposed on the steady two dimensional main flow quantities to obtain the following resultant quantities

$$U, V, W = 0, P, T \text{ and } C \rightarrow U, V, W, P, T \text{ and } \hat{C},$$

$$\hat{U}(x, y, z) = U(x, y) + u'(x, y, z),$$

$$\hat{V}(x, y, z) = V(x, y) + v'(x, y, z),$$

$$\hat{W}(x, y, z) = w'(x, y, z),$$

$$\hat{P}(x, y, z) = P(x, y) + p'(x, y, z),$$

$$\hat{T}(x, y, z) = T(x, y) + t'(x, y, z),$$

$$\hat{C}(x, y, z) = C(x, y) + c'(x, y, z)$$

The disturbance quantities are considered to be dependent on the streamwise coordinate x in addition to normal y , spanwise (z) coordinates. This is in contrast to most of the previous studies in which the disturbances are taken to be independent of x . The resultant quantities given by eq. (18) satisfy the continuity equation, the Navier-Stokes equations, the energy equation and the mass diffusion equation for incompressible steady three-dimensional natural convection flow over non-isothermal inclined flat plate under simultaneous thermal and mass diffusion. Let us substitute eq. (18) into the governing equations. Subtracting the two dimensional main flow and linearizing the main flow quantities, we get

$$\partial u' / \partial x + \partial v' / \partial y + \partial w' / \partial z = 0,$$

$$u' \partial U / \partial x + U \partial u' / \partial x + v' \partial U / \partial y + V \partial u' / \partial y$$

$$= -\frac{1}{\rho} \frac{\partial p'}{\partial x} + \nu \Delta^2 u' + g \beta \sin \phi t' + g \beta^* \sin \phi c'$$

$$u' \partial V / \partial x + U \partial v' / \partial x + v' \partial V / \partial y + V \partial v' / \partial y$$

$$= -\frac{1}{\rho} \frac{\partial p'}{\partial y} + \nu \Delta^2 v' + g \beta \cos \phi t' + g \beta^* \cos \phi c'$$

$$U \partial w' / \partial x + V \partial w' / \partial y = -\frac{1}{\rho} \frac{\partial p'}{\partial z} + \nu \Delta^2 w'$$

$$u' \partial T / \partial x + U \partial t' / \partial x + v' \partial T / \partial y + V \partial t' / \partial y = K \Delta^2 t',$$

$$u' \partial C / \partial x + U \partial c' / \partial x + v' \partial C / \partial y + V \partial c' / \partial y = D \Delta^2 c'$$

where $\Delta^2 = \frac{\partial^2}{\partial x^2} + \frac{\partial^2}{\partial y^2} + \frac{\partial^2}{\partial z^2}$ is the Laplacian operator

Since the disturbances are confined within the boundary layer of main flow, (the so called bottling effect proposed by Haaland and Sparrow [11]), the disturbances will have all the scales different from those of main flow field [27,28]. To this, the disturbance equations are first non-dimensionalized by introducing the following dimensionless quantities

$$X = x/L, Y = y/\epsilon L, Z = z/\epsilon L,$$

where $\epsilon = \left(Gr_{L,t} \cos \phi / 5 \right)^{-1/5}$ and

$$Gr_{L,t} = \left(g \beta (T_w(L) - T_\infty) L^3 \right) / \nu^2.$$

$Gr_{L,t}$ is the Grashof number based on characteristic length $L(x)$. If $L(x) = x$, then $Y = \eta$ and $Gr_{L,t} = Gr_{x,t}$. Other main

variables are scaled as:

$$\begin{aligned} L^+ &= (U^+ L) / V^+, \quad V^+ = V \epsilon L / V^+, \quad \theta = (T - T_\infty) / (T_w(x) - T_\infty), \\ \lambda &= (C - C_\infty) / (C_w(x) - C_\infty), \end{aligned} \quad (26)$$

where L^+, V^+, θ and λ and their derivatives with respect to X and Y are of the order of 1. Similarly, the disturbance quantities are scaled as

$$\begin{aligned} u^+ &= u' \epsilon^2 L / V^+, \quad v^+ = v' \epsilon^2 L / V^+, \quad w^+ = w' \epsilon^2 L / V^+, \\ p^+ &= p' \epsilon^3 L^2 / \mu V^+, \\ t^+ &= t' / (T_w(x) - T_\infty), \quad c^+ = c' / (C_w(x) - C_\infty), \end{aligned} \quad (27)$$

where u^+, v^+, w^+, p^+ and c^+ and their derivatives with respect to X and Y are of the order of ϵ . Substituting above dimensionless variables (25-27) into eqs. (19-24), we obtain

$$\epsilon \frac{\partial u^+}{\partial X} + \frac{\partial v^+}{\partial Y} + \frac{\partial w^+}{\partial Z} = 0, \quad (28)$$

$$\begin{aligned} u^+ \frac{\partial U^+}{\partial X} + U^+ \frac{\partial u^+}{\partial X} + v^+ \frac{\partial U^+}{\partial Y} + V^+ \frac{\partial u^+}{\partial Y} \\ + \epsilon^2 \frac{\partial^2 u^+}{\partial X^2} + \epsilon^2 \frac{\partial^2 u^+}{\partial X \partial Y} + \frac{\partial^2 u^+}{\partial Y^2} + \frac{\partial^2 u^+}{\partial Z^2} \\ + \frac{5}{\epsilon} \tan \phi (t^+ + N c^+), \end{aligned} \quad (29)$$

$$\begin{aligned} u^+ \frac{\partial V^+}{\partial X} + U^+ \frac{\partial v^+}{\partial X} + v^+ \frac{\partial V^+}{\partial Y} + V^+ \frac{\partial v^+}{\partial Y} \\ + \epsilon^2 \frac{\partial^2 v^+}{\partial X^2} + \epsilon^2 \frac{\partial^2 v^+}{\partial X \partial Y} + \frac{\partial^2 v^+}{\partial Y^2} + \frac{\partial^2 v^+}{\partial Z^2} \\ + \frac{5}{\epsilon} (t^+ + N c^+), \end{aligned} \quad (30)$$

$$\begin{aligned} U^+ \frac{\partial w^+}{\partial X} + V^+ \frac{\partial w^+}{\partial Y} \\ + \epsilon^2 \frac{\partial^2 w^+}{\partial X^2} + \epsilon^2 \frac{\partial^2 w^+}{\partial X \partial Y} + \frac{\partial^2 w^+}{\partial Y^2} + \frac{\partial^2 w^+}{\partial Z^2}, \end{aligned} \quad (31)$$

$$\begin{aligned} u^+ \frac{\partial \theta}{\partial X} + U^+ \frac{\partial \theta}{\partial X} + v^+ \frac{\partial \theta}{\partial Y} + V^+ \frac{\partial \theta}{\partial Y} \\ + \frac{1}{Pr} \left[\epsilon^2 \frac{\partial^2 \theta}{\partial X^2} + \epsilon^2 \frac{\partial^2 \theta}{\partial X \partial Y} + \frac{\partial^2 \theta}{\partial Y^2} + \frac{\partial^2 \theta}{\partial Z^2} \right], \end{aligned} \quad (32)$$

$$\begin{aligned} u^+ \frac{\partial \lambda}{\partial X} + U^+ \frac{\partial \lambda}{\partial X} + v^+ \frac{\partial \lambda}{\partial Y} + V^+ \frac{\partial \lambda}{\partial Y} \\ + \frac{1}{Sc} \left[\epsilon^2 \frac{\partial^2 \lambda}{\partial X^2} + \epsilon^2 \frac{\partial^2 \lambda}{\partial X \partial Y} + \frac{\partial^2 \lambda}{\partial Y^2} + \frac{\partial^2 \lambda}{\partial Z^2} \right] \end{aligned} \quad (33)$$

The terms $v^+ \frac{\partial U^+}{\partial Y}$ and $\frac{5}{\epsilon} \tan \phi (t^+ + N c^+)$ in eq. (29), the term $\frac{5}{\epsilon} (t^+ + N c^+)$ in eq. (30) and terms $v^+ \frac{\partial \theta}{\partial Y}$ and $v^+ \frac{\partial \lambda}{\partial Y}$ in eqs. (32) and (33) are larger than the other terms in corresponding equations by at least an order of $1/\epsilon$. This means that the (X, Y, Z) variables as defined in eq. (25) are not appropriate normalization scales for the disturbances. Therefore, by rescaling the coordinates for the disturbance quantities and the disturbance pressure with the form

$$(\bar{X}, \bar{Y}, \bar{Z}, \bar{p}^+) = (X, Y, Z, p^+) \epsilon^{-1/2}, \quad (34)$$

we obtain

$$\epsilon \frac{\partial u^+}{\partial \bar{X}} + \frac{\partial v^+}{\partial \bar{Y}} + \frac{\partial w^+}{\partial \bar{Z}} = 0 \quad (35)$$

$$\begin{aligned} \epsilon u^+ \frac{\partial U^+}{\partial \bar{X}} + \epsilon^{3/2} U^+ \frac{\partial u^+}{\partial \bar{X}} + v^+ \frac{\partial U^+}{\partial \bar{Y}} + \epsilon^{3/2} V^+ \frac{\partial u^+}{\partial \bar{Y}} \\ = -\epsilon^2 \frac{\partial^2 u^+}{\partial \bar{X}^2} + \epsilon^2 \frac{\partial^2 u^+}{\partial \bar{X} \partial \bar{Y}} + \frac{\partial^2 u^+}{\partial \bar{Y}^2} + \frac{\partial^2 u^+}{\partial \bar{Z}^2} \\ + 5 \tan \phi (t^+ + N c^+), \end{aligned} \quad (36)$$

$$\begin{aligned} \epsilon^2 u^+ \frac{\partial V^+}{\partial \bar{X}} + \epsilon^{3/2} U^+ \frac{\partial v^+}{\partial \bar{X}} + \epsilon v^+ \frac{\partial V^+}{\partial \bar{Y}} + \epsilon^{3/2} V^+ \frac{\partial v^+}{\partial \bar{Y}} \\ = -\epsilon \frac{\partial^2 v^+}{\partial \bar{Y}^2} + \epsilon^2 \frac{\partial^2 v^+}{\partial \bar{X}^2} + \frac{\partial^2 v^+}{\partial \bar{Y}^2} + \frac{\partial^2 v^+}{\partial \bar{Z}^2} \\ + 5 (t^+ + N c^+), \end{aligned} \quad (37)$$

$$\begin{aligned} \epsilon^{3/2} U^+ \frac{\partial w^+}{\partial \bar{X}} + \epsilon^{3/2} V^+ \frac{\partial w^+}{\partial \bar{Y}} = -\epsilon \frac{\partial^2 w^+}{\partial \bar{Z}^2} + \epsilon^2 \frac{\partial^2 w^+}{\partial \bar{X}^2} \\ + \frac{\partial^2 w^+}{\partial \bar{Y}^2} + \frac{\partial^2 w^+}{\partial \bar{Z}^2}, \end{aligned} \quad (38)$$

$$\begin{aligned} \epsilon u^+ \frac{\partial \theta}{\partial \bar{X}} + \epsilon^{3/2} U^+ \frac{\partial \theta}{\partial \bar{X}} + v^+ \frac{\partial \theta}{\partial \bar{Y}} + \epsilon^{3/2} V^+ \frac{\partial \theta}{\partial \bar{Y}} \\ = \frac{1}{Pr} \left[\epsilon^2 \frac{\partial^2 \theta}{\partial \bar{X}^2} + \epsilon^2 \frac{\partial^2 \theta}{\partial \bar{X} \partial \bar{Y}} + \frac{\partial^2 \theta}{\partial \bar{Y}^2} + \frac{\partial^2 \theta}{\partial \bar{Z}^2} \right], \end{aligned} \quad (39)$$

$$\begin{aligned} \epsilon u^+ \frac{\partial \lambda}{\partial \bar{X}} + \epsilon^{3/2} U^+ \frac{\partial \lambda}{\partial \bar{X}} + v^+ \frac{\partial \lambda}{\partial \bar{Y}} + \epsilon^{3/2} V^+ \frac{\partial \lambda}{\partial \bar{Y}} \\ = \frac{1}{Sc} \left[\epsilon^2 \frac{\partial^2 \lambda}{\partial \bar{X}^2} + \epsilon^2 \frac{\partial^2 \lambda}{\partial \bar{X} \partial \bar{Y}} + \frac{\partial^2 \lambda}{\partial \bar{Y}^2} + \frac{\partial^2 \lambda}{\partial \bar{Z}^2} \right] \end{aligned} \quad (40)$$

The terms $\epsilon^2 \frac{\partial u^*}{\partial \bar{X}}, \epsilon^2 \frac{\partial \bar{p}^*}{\partial \bar{X}}, \epsilon^2 \frac{\partial^2 u^*}{\partial \bar{X}^2}, \epsilon^2 \frac{\partial^2 v^*}{\partial \bar{X}^2}, \epsilon^2 \frac{\partial^2 w^*}{\partial \bar{X}^2}, \epsilon^2 \frac{\partial^2 t^*}{\partial \bar{X}^2}$ and $\epsilon^2 \frac{\partial^2 c^*}{\partial \bar{X}^2}$ in eqs (35-40) are smaller than the rest of the terms in their respective equations. They can be omitted. The omission of these lowest order terms in the disturbance equations is consistent with the level of approximation of the main flow. Deleting above mentioned terms and using eq (34), the disturbance equations are reduced to

$$\frac{\partial u^*}{\partial Y} + \frac{\partial w^*}{\partial Z} = 0, \quad (41)$$

$$u^* \frac{\partial U^*}{\partial X} + U^* \frac{\partial u^*}{\partial X} + \left(Gr_{Li} \cos \phi / 5 \right)^{1/5} v^* \frac{\partial U^*}{\partial Y} + V^* \frac{\partial u^*}{\partial Y} = \frac{\partial^2 u^*}{\partial Y^2} + \frac{\partial^2 u^*}{\partial Z^2} + S \left(Gr_{Li} \cos \phi / 5 \right)^{1/5} \tan \phi (t^* + Nc^*), \quad (42)$$

$$\left(Gr_{Li} \cos \phi / 5 \right)^{1/5} u^* \frac{\partial V^*}{\partial X} + U^* \frac{\partial v^*}{\partial X} + v^* \frac{\partial V^*}{\partial Y} + V^* \frac{\partial v^*}{\partial Y} = - \frac{\partial p^*}{\partial Y} + \frac{\partial^2 v^*}{\partial Y^2} + \frac{\partial^2 v^*}{\partial Z^2} + S \left(Gr_{Li} \cos \phi / 5 \right)^{1/5} (t^* + Nc^*), \quad (43)$$

$$U^* \frac{\partial w^*}{\partial X} + V^* \frac{\partial w^*}{\partial Y} = - \frac{\partial p^*}{\partial Z} + \frac{\partial^2 w^*}{\partial Y^2} + \frac{\partial^2 w^*}{\partial Z^2}, \quad (44)$$

$$u^* \frac{\partial \theta^*}{\partial X} + U^* \frac{\partial t^*}{\partial X} + v^* \frac{\partial \theta^*}{\partial Y} \left(Gr_{Li} \cos \phi / 5 \right)^{1/5} + V^* \frac{\partial t^*}{\partial Y} = \frac{1}{Pr} \left[\frac{\partial^2 t^*}{\partial Y^2} + \frac{\partial^2 t^*}{\partial Z^2} \right], \quad (45)$$

$$u^* \frac{\partial \lambda^*}{\partial X} + U^* \frac{\partial c^*}{\partial X} + \left(Gr_{Li} \cos \phi / 5 \right)^{1/5} v^* \frac{\partial \lambda^*}{\partial Y} + V^* \frac{\partial c^*}{\partial Y} = \frac{1}{Sc} \left[\frac{\partial^2 c^*}{\partial Y^2} + \frac{\partial^2 c^*}{\partial Z^2} \right] \quad (46)$$

Now, the pressure terms in eqs (43) and (44) are eliminated by cross differentiation and subtraction. The resulting equation is then differentiated with respect to Z once and the substitution $\frac{\partial w^*}{\partial Z} = - \frac{\partial v^*}{\partial Y}$ from the continuity equation is employed

to remove the terms involving the function w^* and its derivative. This sequence of operations will yield four equations for the disturbance quantities u^*, v^*, t^* and c^* . For the non-parallel flow model, above quantities are expressed as

$$(u^*, v^*, t^*, c^*)$$

$$= [u_0(X, Y), v_0(X, Y), t_0(X, Y), c_0(X, Y)] \exp(i a \bar{Z})$$

where a is the dimensional azimuthal wave number of the disturbances. Thus, the longitudinal vortex rolls are taken to be periodic in the spanwise Z direction with amplitude functions depending on both X and Y . Substituting eq (47) into eqs (42-45) the combined form of eqs (43) and (44) as described above and eqs (45, 46) along with introducing the coordinate transformation from (X, Y) to (X, η) through the following relationship

$$Y = X^{2/5} \eta, \quad \frac{\partial}{\partial Y} = X^{-2/5} \frac{\partial}{\partial \eta}, \quad Y \frac{\partial}{\partial Y} = \eta \frac{\partial}{\partial \eta}$$

and writing

$$\alpha^2 = a^2 X^{4/5}, \quad u = u_0, \quad v = v_0, \quad c = c_0 X^{1/5}, \quad t = t_0 X^{1/5}$$

we obtain the following system of partial differential equations for the disturbance amplitude functions u, v, t and c

$$D^2 u + \bar{a}_1 D u + a_2 u + a_3 v + a_4 (t + Nc) = 5 f X \frac{d u}{d X}$$

$$D^4 v + b_1 D^3 v + b_2 D^2 v + b_3 D v + b_4 v + b_5 (t + Nc) = 5 f' X \frac{d v}{d X}$$

$$= 5 f' X \frac{\partial}{\partial X} (D^2 v) + 5 f' X \frac{\partial}{\partial X} (D v) - 5 \alpha^2 f X \frac{d v}{d X}$$

$$D^2 t + \bar{d}_1 D t + \bar{d}_2 t + \bar{d}_3 u + \bar{d}_4 v = 5 Pr f X \frac{d t}{d X}$$

$$D^2 c + e_1 D c + e_2 c + e_3 u + e_4 v = 5 Sc f X \frac{d c}{d X}$$

The corresponding boundary conditions are

$$u = v = Dv = t = c = 0, \quad \text{at } \eta = 0 \quad \text{and } \eta = \infty$$

In eqs (50-53), $D^n = d^n / d\eta^n$ and the boundary conditions arise from the vanishing of the disturbances at the wall and the free stream in which $Dv = 0$, results from the continuity equation $\frac{\partial v}{\partial Y} + \frac{\partial w}{\partial Z} = 0$ along with $w^* = 0$ at $\eta = 0$ and $\eta = \infty$. The main flow and thermal fields are expressed as functions of (ξ, η) , it is convenient to express the disturbance amplitude functions u, v, t and c as a function of (ξ, η) . Transforming (X, η) to (ξ, η) through the relationship

$$X \frac{\partial}{\partial X} = X \frac{\partial}{\partial \xi} \frac{d \xi}{d X} + X \frac{\partial}{\partial \eta} \frac{d \eta}{d X}$$

$$= \frac{\partial}{\partial \xi} \left(n + \frac{3}{5} \right) \xi + \frac{\partial}{\partial \eta} \left(n - \frac{2}{5} \right) \eta, \quad (55)$$

obtain the following system of partial differential equations for the disturbance amplitude functions u , v , t and c in case of $\tau f, \mu = 0$

$$D^2 u + a_1^* D u + a_2^* u + a_3^* v + a_4^* (t + Nc) = 3f \xi \frac{\partial u}{\partial \xi}, \quad (56)$$

$$D^4 v + b_1^* D^3 v + b_2^* D^2 v + b_3^* D v + b_4^* v + b_5^* u + b_6^* (t + Nc)$$

$$+ 3f \xi \frac{\partial}{\partial \xi} D^2 v + 3f \xi \frac{\partial}{\partial \xi} D v - 3f \alpha^2 \xi \frac{\partial v}{\partial \xi}, \quad (57)$$

$$D^2 t + d_1^* D t + d_2^* t + d_3^* u + d_4^* v = 3Pr f \xi \frac{\partial t}{\partial \xi}, \quad (58)$$

$$D^2 c + e_1^* D c + e_2^* c + e_3^* u + e_4^* v = 3Sc f \xi \frac{\partial c}{\partial \xi}, \quad (59)$$

Eq. (56-59) along with their boundary conditions (54) represent the mathematical system for the stability problem. Since (56-59) are partial differential equations, the boundary conditions as given by (54) are not sufficient if ξ derivatives of u and v are not set equal to zero. The well known methods are used to solve such a system of equations as the local similarity and local non-similarity methods. When the terms on the right side of eqs. (56-59) are deleted, the resulting equations along with boundary conditions (54) provide a system of equations for the local similarity non-parallel flow model. For this system of equations for the local non-similarity non-parallel flow model, we introduce

$$\sigma = \partial u / \partial \xi, \omega = \partial v / \partial \xi, \tau = \partial t / \partial \xi, s = \partial c / \partial \xi \quad (60)$$

Eq. (56-59) and boundary conditions (54) are then differentiated with respect to ξ once to obtain equations for σ and s . Neglecting the terms $\partial \sigma / \partial \xi$, $\partial \omega / \partial \xi$, $\partial \tau / \partial \xi$, $\partial s / \partial \xi$ we find a system of homogenous ordinary differential equations for the disturbance amplitude functions u , v , t , c , σ and s .

$$D^2 u + a_1 D u + a_2 u + a_3 v + a_4 (t + Nc) + a_5 \sigma = 0, \quad (61)$$

$$D^4 v + b_1 D^3 v + b_2 D^2 v + b_3 D v + b_4 v + b_5 u + b_6 (t + Nc) + b_7 D^2 \omega + b_8 D \omega + b_9 \omega = 0, \quad (62)$$

$$D^2 t + d_1 D t + d_2 t + d_3 u + d_4 v + d_5 \tau = 0, \quad (63)$$

$$D^2 c + e_1 D c + e_2 c + e_3 u + e_4 v + e_5 s = 0, \quad (64)$$

$$D^2 \sigma + f_1 D \sigma + f_2 \sigma + f_3 \omega + f_4 (\tau + Ns) + f_5 D u$$

$$+ f_6 u + f_7 v + f_8 (t + Nc) = 0, \quad (65)$$

$$D^4 \omega + g_1 D^3 \omega + g_2 D^2 \omega + g_3 D \omega + g_4 \sigma + g_5 (\tau + Ns) + g_7 D^3 v + g_8 D^2 v + g_9 D v + g_{10} v + g_{11} u + g_{12} (t + Nc) = 0, \quad (66)$$

$$D^2 \tau + h_1 D \tau + h_2 \tau + h_3 \sigma + h_4 \omega + h_5 t + h_6 u + h_7 v + h_8 v = 0, \quad (67)$$

$$D^2 s + j_1 D s + j_2 s + j_3 \sigma + j_4 \omega + j_5 D c + j_6 c + j_7 u + j_8 v = 0, \quad (68)$$

with the boundary conditions

$$u = v = D v = t = c = \sigma = \omega = D \omega = \tau = s = 0 \text{ at } \eta = 0 \text{ and } \eta = \infty \quad (69)$$

The coefficients in eqs. (61)-(68) are defined in the Appendix

The system of coupled differential eqs. (61-68) along with the homogenous boundary conditions (69) forms an eigen value problem of the form

$$E(G_{1/2}, \alpha, Pr, Sc, N, \phi, n) = 0 \quad (70)$$

For given values of exponent n , Prandtl number Pr , Schmidt number Sc , relative buoyancy ratio parameter N , and angle of inclination ϕ , the values of wave number α satisfying above eq. (70) is sought as eigenvalue for a given value of $G_{1/2}$ or the non-similarity parameter ξ .

3. Numerical method of solution

The system of equations for the main flow, thermal and concentration fields, eqs. (8-11) was solved by block elimination method. The details of the technique are omitted here. However, for the treatment of the integrals involving θ , $\partial \theta / \partial \xi$, λ and $\partial \lambda / \partial \xi$ in eq. (8), we introduce

$$G = \int_{\eta}^{\infty} \theta d\eta, \quad H = \int_{\eta}^{\infty} \lambda d\eta \quad (71)$$

which gives rise to two additional equations

$$G' + \theta = 0, \quad G(\xi, \infty) = 0, \quad (72)$$

$$H' + \lambda = 0, \quad H(\xi, \infty) = 0, \quad (73)$$

and eq. (8) simplifies to

$$f''' + (n+3)ff'' - (2n+1)(f')^2 + \xi(\theta + \lambda N) + \frac{1}{\xi}(2-n)\eta(\theta + \lambda N) + \frac{1}{\xi}(4n+2)(G + NH) + \frac{1}{\xi}(n+3)\xi \frac{\partial}{\partial \xi}(G + NH) = (n+3)\xi \left(f' \frac{\partial f'}{\partial \xi} - f'' \frac{\partial f}{\partial \xi} \right) \quad (74)$$

Thus, finite difference solution was performed on eqs (74), (9-11), (72) and (73) to obtain main flow quantities $f, f', f'', \theta, \theta', \lambda, \lambda'$ and their partial derivatives with respect to ξ that are needed in the stability computations and in the determination of local Nusselt number, local Sherwood number and the local wall shear stress. This approach gives a better rate of convergence and hence, reduces the numerical computation time. As the number of first order equations to be solved with the block elimination method is 9, the preparation of the solution algorithm with the recursion formula becomes tedious. So, we use the matrix-solver algorithm (described in chapter 5 [26]).

The equation describing the stability problem, equations (56-59) with their terms on right hand side deleted, the four equations model or of equations (61-68) for the eight equation model, were solved numerically by a finite difference scheme along with Muller's shooting method. The solution method parallels that described in [29]. This eigenvalue problem is best solved by approximating the boundary conditions at $\eta = \eta_\infty$ with the asymptotic solution of eqs (61-68). The asymptotic solutions for u, v, t and c at $\eta = \eta_\infty$ consist of five sets of independent solutions (u_i, v_i, t_i and c_i) with $i=1,2,3,4$ and 5 [30] that can be easily obtained.

In determining the neutral stability curve for given values of Pr, Sc, N, n , and ϕ , the eigenvalue problem is to find the value of α for a specified value of $Gr_{\lambda, t}$. This is done as follows. First, the main flow solution is obtained to provide the coefficients $a_1 - a_8$ for a pre-assigned value of ξ with the given values of Pr, Sc, N, n . With the angle ϕ specified, the parameter $Gr_{\lambda, t} \cos \phi / 5 = (\xi / \tan \phi)^5$ is specified with this known value of $Gr_{\lambda, t}$ and a guessed value of wave number α as the eigen value, the finite difference forms of eqs (61-68) are numerically solved from $\eta = 0$ to $\eta = \infty$ ending with the asymptotic solutions for $u, v, t, c, \sigma, \omega, \tau$ and s . The guessed eigenvalue α is then corrected by Muller shooting method until the boundary conditions at the wall ($\eta = 0$) are satisfied within a certain specified tolerance. This gives a converged α value as the eigenvalue for the given values of n, Pr, Sc, N, ϕ and $Gr_{\lambda, t}$. This completes a solution of the eigenvalue problem. The same process is repeated to obtain different values of the $(\alpha, Gr_{\lambda, t})$ pair in mapping out a neutral stability curve.

Numerical computations were carried out for $Pr = 0.7$ and $Sc = 0.6, 1.2$ with N ranging from -0.5 to 2 . The Schmidt number range covers typically diffusion into air of water vapour ($Sc=0.6$), carbon dioxide (0.94), methanol (0.97) and ethyl benzene (2.01). The neutral stability curves for different values of exponent n ranging from 0 to 1 are plotted. In the calculations, the values of η_∞ were found to depend on the Schmidt number Sc and the N value. For $Sc = 1.2$ and $N = 1.2$, $\eta_\infty = 7$ and for $N = -0.5$, $\eta_\infty = 8$

were found to be sufficient in both the mainflow and stability calculations. Whereas for $Sc = 0.6$, $\eta_\infty = 8$, $N = 1.2$ and $\eta_\infty = 11$ for $N = -0.5$ were required. In the main flow solutions by the finite difference method, variable step sizes were used in the η direction. The step size was increased gradually with increasing ξ and ranged $\Delta \xi = 0.1$ for $0 \leq \xi \leq 1$ to $\Delta \xi = 2.0$ for $\xi > 1$. On the other hand, uniform step size of $\Delta \eta = 0.02$ in the η direction was used in the main flow calculations. In the stability calculations, $\Delta \eta$ was taken to be 0.04 for $0 \leq \eta \leq \eta_\infty$.

4. Results and discussion

Numerical results for the local wall shear stress, the local Nusselt number and the local Sherwood number are shown in terms of $\tau_w (x^2/5\mu\nu) (Gr_{\lambda, t} \cos \phi / 5)^{-1/5}$, $Nu_x (Gr_{\lambda, t} \cos \phi / 5)^{1/5}$ and $Sh_x (Gr_{\lambda, t} \cos \phi / 5)^{-1/5}$ respectively, in Figures 1-3. These figures reveal that above three quantities increase with increasing values of ξ . The wall shear stress and surface heat or mass transfer rates either increase with the increasing angle of inclination for a fixed local thermal Grashof number $Gr_{\lambda, t}$ or increase with the increasing thermal Grashof number for a fixed angle ϕ . Physically, this implies that when the local thermal Grashof number is increased or when the angle ϕ is increased,

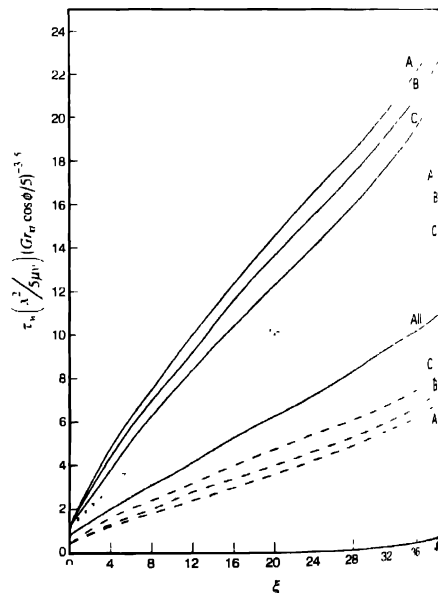


Figure 1 Local wall shear stress results for UWT ($n = 0$). $Pr = 0.7$, $Sc = 0.6, 1.0, 2.0$. $N = 1.0$ ——— $N = -0.5$ - - -

horizontal ($\phi=0$ deg) towards the vertical ($\phi=90$ deg) rotation, the buoyancy forces will become more pronounced. This causes an increase in the wall shear stress and the surface heat or mass transfer rates. This condition will prevail as long as the combined buoyancy forces ($N>0$) from thermal and mass diffusion drive the flow.

For a given value of Schmidt number (Figures 1-3), the wall shear stress and surface heat or mass transfer rates increase with the increasing value of N when $N>0$ i.e. both thermal diffusion and mass diffusion combine to drive the flow. On the other hand, the values of these three quantities become lower, the buoyancy force from mass diffusion opposes the thermal buoyancy force ($N<0$) than those for $N=0$ (no buoyancy force from mass diffusion). In addition, as the Schmidt number increases, both the local wall shear stress and the local Nusselt number increase when $N>0$ and decrease when $N<0$. This is due to the fact that a smaller Schmidt number corresponds to a larger mass diffusion coefficient, which in turn, exerts a larger influence on the flow field and hence, the thermal field. Figure 3 predicts that for a fixed buoyancy ratio parameter, larger Schmidt numbers are associated with larger Schmidt numbers. This surface mass transfer rate increases with the increasing

Schmidt number. This is because a large Schmidt number provides a thinner concentration boundary layer thickness relative to the flow boundary layer thickness, thereby resulting in a larger concentration gradient at the wall and hence, an enhancement in the surface mass transfer rate. This trend is analogous to the heat transfer process in which the surface heat transfer rate increases as the Prandtl number increases.

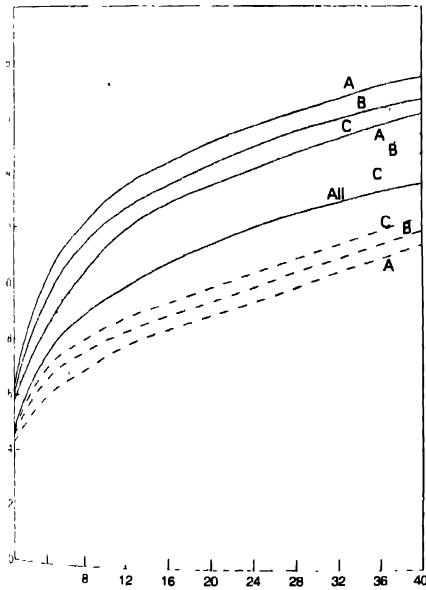


Figure 2. Local Nusselt number results for UWT ($n=0$), $Pr=0.7$. Values for curve A = 0.6, B = 1.0, C = 2.0. $N=2.0$ — $N=1.0$ - - - $N=0$. . .

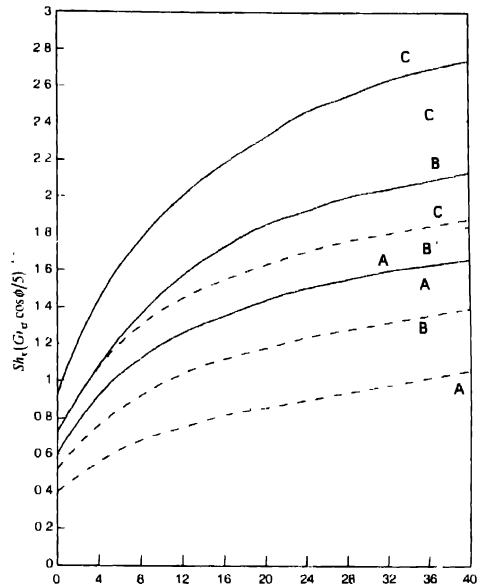


Figure 3. Local Sherwood number results for UWT ($n=0$), $Pr=0.7$. Values of Sh_x for curve A = 0.6, B = 1.0, C = 2.0. $N=2.0$ — $N=1.0$ - - - $N=0.5$ - - -

The local wall shear stress and local Nusselt number as a function of ξ are shown in Figures 4 and 5 for values of exponent n of 0, 1/3 and 1, for both $Pr=0.7$ and 7.0. As can be seen from these figures, for a given value of n , both the wall shear stress and surface heat transfer rate increase with the increasing value of ξ . These two quantities increase with the increasing angle of inclination ϕ from the horizontal for a given value of local Grashof number $Gr_{x,t}$ or with the increasing local Grashof number $Gr_{x,t}$ for a given inclination angle ϕ . In addition, the surface heat transfer rate (Figure 5) increases with an increase in n for a given value of ξ with a larger Pr yielding a higher transfer rate.

To show the variations of local Nusselt number Nu_x and the local Sherwood number Sh_x with the local thermal Grashof

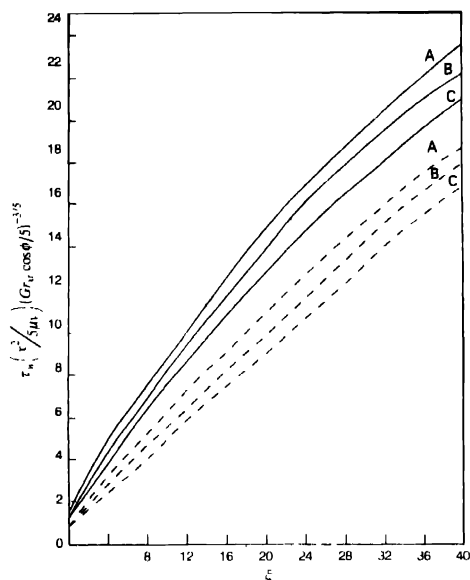


Figure 4. Local wall shear stress results for $T_w(x) - T_\infty = \alpha x^n$, $Sc = 0.6$, $N = 2.0$. Values of n for curve A = 0.0, B = 1/3, C = 1.0 $Pr = 0.7$ — $Pr = 7.0$ ---

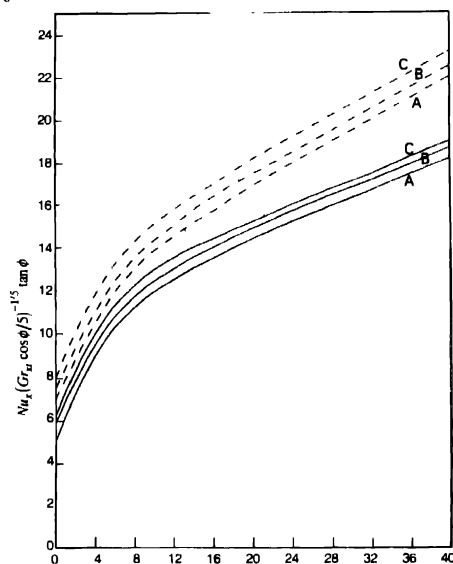


Figure 5. Local Nusselt number results for $T_w(x) - T_\infty = \alpha x^n$. Values of n for curve A = 0.0, B = 1/3, C = 1.0 $Pr = 0.7$ — $Pr = 7.0$ ---

number Gr_{x1} , the angle of inclination ϕ and the buoyancy ratio parameter N . Figures 6 and 7 are drawn. It can be seen that both Nu_x and Sh_x increase with the increasing values of Gr_{x1} , ϕ and N . The results for different angles of inclination ($\phi = 15$ to 90 deg) are shown in the diagram. Angle of inclination $\phi = 90$ is not considered because in this case, the plate will be in vertical position.

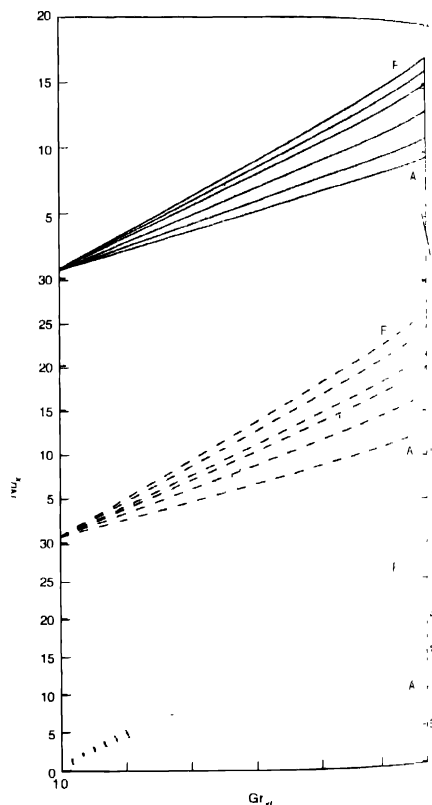


Figure 6. Local Nusselt number versus local thermal Grashof number, various angle of inclination, $n = 0$, $Pr = 0.7$, $Sc = 1.0$, $N = 2.0$ (—) $N = 0.5$ (---). Values of ϕ for A = 0, B = 15, C = 30, D = 45, E = 60, F = 75 deg.

Neutral stability curves and critical wave and Grashof numbers were obtained for various angles of inclination ranging from 0 deg to 75 deg. Representative neutral stability curves are plotted in Figure 8 for $Pr = 0.7$ and $Sc = 1.0$ for different values of $\phi = 0, 30$ and 60 deg. It is seen from the figures that at a fixed value of N , as the angle ϕ increases from 0 deg

... stability curve shifts right upward indicating a stabilization of the main flow to the vortex mode of instability at a higher wave number. On the other hand, at a given angle of inclination ϕ , as buoyancy ratio parameter increases from a negative to a positive value, the neutral stability curve shifts upward indicating destabilization of the flow at a larger wave number. Physically, this implies that a larger N value gives rise to a stronger effect of combined buoyancy forces, which in turn contributes to a less stable flow. Figure 8 reveals that for a

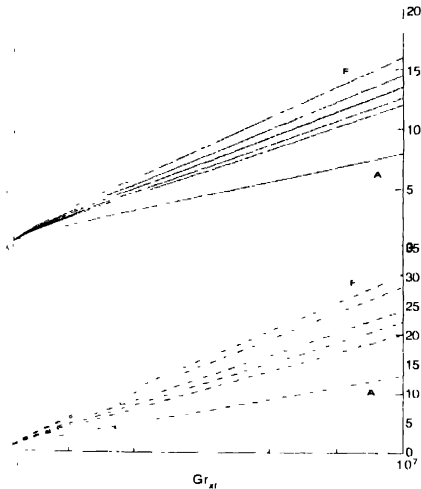


Figure 8. Local Sherwood number versus local thermal Grashof number for various angles of inclination, $\phi = 0$, $Pr = 0.7$, $Sc = 1.0$, $N = 2$ (—), $N = 1$ (---), $N = 0$ (---), $N = -0.5$ (---). Values of ϕ for A = 0, B = 15, C = 30, D = 45, E = 60. I = 1.

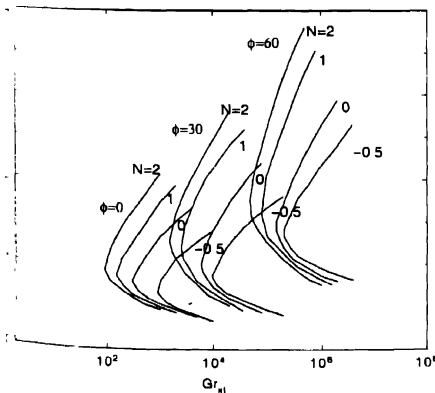


Figure 9. Representative neutral stability curves for $\phi = 0, 30, 60$ deg. $Pr = 0.7$.

fixed angle ϕ , the locus of critical points (i.e. the points of minimum thermal Grashof numbers) on the neutral stability curves for different N values, forms a straight line.

The effect of Schmidt number on the vortex instability of the flow, neutral stability curves for $Pr = 0.7$ and $Sc = 0.6, 1$ and 2 at a fixed angle $\phi = 30$ deg. with $N = -0.5, 0, 1$ and 2 are shown in Figure 9. The critical points on the neutral stability curves for different values of buoyancy ratio parameters N form a straight line, which is different for a different Schmidt number. The relative position of critical points for different Schmidt numbers appears to shift with a change in the N value. In general, a decrease in the N value contributes to the stabilization of flow and a decrease in the Schmidt number from 1 to 0.6 for a fixed N value tends to stabilize the flow when $N > 0$ and to destabilize the flow when $N < 0$. However, no such definite trend is available when Schmidt number is increased from 1 to 2 ($N < 0$). These results follow from a very complicated interactions of the two buoyancy effects through velocity to the diffusion mechanism on the stability characteristics of the flow.

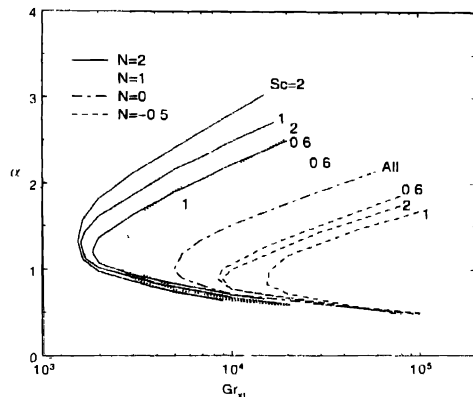


Figure 9. Representative neutral stability curves for $\phi = 30$ deg., $Pr = 0.7$.

The critical thermal Grashof numbers $Gr_{x,l}^*$ and critical wave number α^* at various angles of inclination ϕ are listed in Table 1 for $Pr = 0.7$ and $Sc = 0.6, 1$ and 2 with $N = -0.5, 0, 1$ and 2 . The angular variation of these critical thermal Grashof numbers are also plotted in Figure 10. From the table and figure, it is observed that an inclined natural convection flow with mass diffusion becomes less susceptible to the vortex mode of instability as the plate is tilted from the horizontal towards the vertical orientation. The flow is the most susceptible to the vortex mode of instability, when the plate is horizontal and this susceptibility diminishes as ϕ increases and thermal Grashof number becomes

Table 1. Critical thermal Grashof numbers and wave numbers for Pr

$\alpha(\text{deg})$	$Sc = 0.6$							
	$N=2$		$N=1$		$N=0$		$N=-0.5$	
	Gr_{crit}^*	α^*	Gr_{crit}^*	α^*	Gr_{crit}^*	α^*	Gr_{crit}^*	α^*
0	112	0.833	204	0.842	300.08	0.799	709	0.698
15	457	1.065	737	0.985	1280	0.898	2295	0.802
30	1862.17	1.212	2793.3	1.118	6250.5	0.949	8585.73	0.912
45	8832	1.394	13013	1.294	25580	1.112	40465	1.052
60	59862	1.666	88410	1.545	145709	1.456	274165	1.252
75	1129962	2.073	1670010	2.01	3118109	1.882	4916000	1.632
$Sc = 1.0$								
0	91.029	0.912	150.99	0.865	300.08	0.799	920.223	0.705
15	363	1.06	584	0.985	1280	0.898	3070	0.795
30	1526.42	1.249	2531.94	1.146	6250.5	0.949	9644.98	0.855
45	7266	1.458	11501	1.332	25580	1.112	47944	0.984
60	50867	1.625	81380	1.559	145709	1.456	200901	1.399
75	946067	2.182	1473380	2.052	3118109	1.882	6081901	1.744
$Sc = 2.0$								
0	70	0.9505	93	0.91	300.08	0.799	959	0.678
15	325	1.1215	508	1.062	1280	0.898	3053	0.775
30	1460.48	1.3115	2389.94	1.212	6250.5	0.949	9043.87	0.885
45	7430	1.5525	12279	1.417	25580	1.112	38013	1.021
60	52290	1.894	86279	1.697	145109	1.456	244513	1.208
75	998090	2.481	1639979	2.245	3118109	1.882	4580513	1.565

∞ when the plate is vertical. This is because when the plate is vertical, there is no buoyancy force component that acts normal to the plate and as a result, vortex mode of instability does not take place. The instability of the flow is seen to be affected strongly by the buoyancy force from mass diffusion. The flow becomes less or more stable to the vortex mode of instability, depending on whether the buoyancy force from mass diffusion assists ($N > 0$) or opposes ($N < 0$) the thermal buoyancy force.

A comparison between the present vortex instability results for the inclined plate with the wave instability results for the horizontal and vertical plate (Table 2) indicates that the first onset of the instability of the flow is due to the vortex mode of disturbances when the plate is horizontal, whereas in a vertical plate, it is due to wave mode of disturbances. Thus, a crossover from vortex to the wave mode of instability is expected to occur as the plate is tilted from the horizontal towards the vertical position. However, an accurate assessment of the inclination angles at which cross over takes place cannot be made at present due to lack of wave instability results for inclined free convection flows with combined buoyancy mode of thermal and mass diffusion. There is no experimental instability data available for

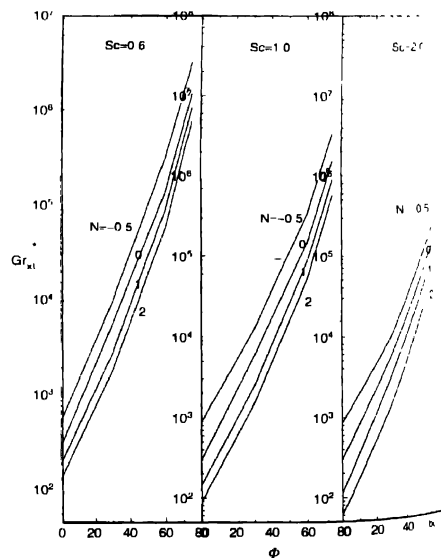


Figure 10. Critical thermal Grashof number versus angle of inclination

Table 2 Comparison of critical values with those obtained by previous works on vortex/wave instability

Author and Gebhart [9] Natural convection	$5[(1+N) Gr_w^*/5]^{1/4}$	N	Gr_w^*
$N_c = 0.7$	4.9	2	1.51×10^5
	5.3	1	3.35×10^5
instability	6.4	0	1.72×10^6
	7.7	-0.5	8.66×10^6
Author and Gebhart [12] Natural convection	$4(Gr_w^*/4)^{1/4}$	N	Gr_w^*
$N_c = 0.94$	6.0	0.5	2.03×10^5
	6.6	0	2.96×10^5
instability	7.3	0.2	4.49×10^6
Author and [17] Natural convection	α^* (Critical wave number)	N	Gr_w^*
$N_c = 0.6$	0.702	2	132
	0.652	1	191
	0.583	0	340
	0.516	-0.5	544
Author and [21] Experiment	$\alpha_c^* = 2.17-4.97$ $\alpha^* = 0.895-2.049$ $N_c, \lambda = (0.16-0.31) Re_c^{1/4}$		$Gr_w/Re_c^{3/2} = 46-110$
Author and analysis	α^* (Critical wave number)	N	Gr_w^*
$N_c = 0.6$	0.853	2	112
on surface	0.842	1	204
on surface	0.799	0	300.08
parallel flow	0.698	0.5	709
Author and Kim [32] Experiments	α^* Pr = 0.7 [UWT]		Gr_w^*
	0.33204-0.42970		$0.35-11.37 \times 10^5$
Author and [25] Parallel flow	α^*		Gr_w^*
Pr = 0	0.68803		834.52

Values as expressed in original papers

comparison with the present analysis except for the case a)

Conclusion

In this paper, non-parallel vortex instability characteristics of buoyancy induced flows that result from simultaneous diffusion of heat and mass in laminar boundary layers adjacent to horizontal and inclined surfaces with a power law variation in the temperature, has been investigated analytically by extending the linear non-parallel flow theory. The analysis is restricted to situations in which low concentration level exists such that diffusion-thermo/thermo-diffusion effects and the interfacial velocities due to mass diffusion are neglected. The present non-parallel flow model which takes into account the

streamwise dependence of the disturbances, predicts large critical Grashof numbers in comparison to parallel flow model, thus bringing closer agreement to available experimental data. When the buoyancy force from mass diffusion assists the thermal buoyancy force, the heat/mass transfer rates increase and the flow becomes less stable to the vortex mode of instability. These trends are reversed when the two buoyancy forces oppose each other. As the angle of inclination from the horizontal is increased, the buoyancy force effects become more pronounced. This gives rise to an increase in the surface heat or mass transfer rates, but to a stabilization of the main flow to the vortex mode of disturbance.

References

- [1] B. Gebhart and L. Pera *Int. J. Heat Mass Transfer* **14**, 2025 (1971).
- [2] L. Pera and B. Gebhart *Int. J. Heat Mass Transfer* **15**, 269 (1972).
- [3] T. S. Chen and C. F. Yuh *Numer. Heat Transfer* **2**, 233 (1979).
- [4] T. S. Chen *et al.* *Int. J. Heat Mass Transfer* **29**(10), 1465 (1986).
- [5] R. A. Kahawita and R. N. Meroney *Int. J. Heat Mass Transfer* **17**, 541 (1974).
- [6] S. E. Haaland and E. M. Sparrow *Int. J. Heat Mass Transfer* **16**, 2355 (1973).
- [7] P. A. Iyer and R. E. Kess *Int. J. Heat Mass Transfer* **17**, 517 (1974).
- [8] P. R. Nachtsheim NASA TN D 2089 (1963).
- [9] L. Pera and B. Gebhart *Int. J. Heat Mass Transfer* **16**, 1147 (1973).
- [10] G. J. Hwang and K. C. Chen *Canad. J. Chem. Engng* **51**, 659 (1973).
- [11] S. E. Haaland and E. M. Sparrow *ASME J. Heat Transfer* **96**, 405 (1973).
- [12] A. R. Boura and B. Gebhart *AIChE J.* **22**, 94 (1976).
- [13] T. S. Chen and K. L. Tzuoo *ASME J. Heat Transfer* **104**, 637 (1982).
- [14] H. R. Lee, T. S. Chen and B. F. Armaly *Int. J. Heat Mass Transfer* **34**, 305 (1991).
- [15] B. Gebhart *ASME J. Fluid Engng* **101**, 5 (1979).
- [16] J. R. Lloyd and E. M. Sparrow *J. Fluid Mech.* **42**, 465 (1970).
- [17] T. S. Chen, K. L. Tzuoo and A. Moutsoglou *J. Heat Transfer* **105**, 774 (1983).
- [18] K. Fujimura and R. E. Kelly *J. Fluid Mech.* **246**, 545 (1993).
- [19] H. Shaikatullah and B. Gebhart *Int. J. Heat Mass Transfer* **21**, 1481 (1978).

- [20] G S H Lock, C Gort and G R Pond *Appl. Sci. Res.* **18** 171 (1997)
- [21] R S Wu and K C Cheng *Int. J. Heat Mass Transfer* **19** 907 (1976)
- [22] H C Tien, T S Chen and B F Aimaly *Numer. Heat Transfer* **9** 697 (1986)
- [23] K Chen and M M Chen *J. Heat Transfer* **106** 284 (1984)
- [24] J Y Yoo, P Park, C K Chou and S T Rao *J. Heat Mass Transfer* **30** 927 (1987)
- [25] H R Lee, T S Chen and B F Aimaly *Int. J. Heat Mass Transfer* **33** 2019 (1990)
- [26] T Cebeci and J Cousteix *Modelling and Computation of Boundary Layer Flows* (Berlin: Springer-Verlag) (1999)
- [27] C T Hsu, P Cheng and G M Homay *Int. J. Heat Mass Transfer* **21** 1221 (1978)
- [28] C T Hsu and P Cheng *J. Heat Transfer* **101** 660 (1979)
- [29] S L Lee, T S Chen and B F Aimaly *Numer. Heat Transfer* **10** 01 (1986)
- [30] A Moutsoglou, T S Chen and K C Cheng *J. Heat Transfer* **103** 257 (1981)
- [31] R R Gilpin, H Imuta and K C Cheng *J. Heat Transfer* **100** 71 (1978)
- [32] K C Cheng and Y W Kim *J. Heat Transfer* **110** 608 (1988)

Nomenclature

- a = dimensionless wave number of disturbance
- A, B = real constants
- C = species concentration
- D = diffusion coefficient
- D'' = $d''/d\eta''$, differential operator
- f = reduced stream function
- g = gravitational acceleration
- $Gr_{\lambda T}$ = thermal Grashof number
- $Gr_{\lambda c}$ = Grashof number for mass diffusion
- K = thermal conductivity of fluid
- L = x , characteristics length
- n = exponent in the power law variation of wall temperature
- N = buoyancy ratio parameter
- Nu_{λ} = local Nusselt number
- p' = perturbation pressure
- P = main flow pressure
- Pr = ν/k Prandtl number
- s = $\partial c/\partial \xi$
- Sc = ν/D Schmidt number
- Sh_{λ} = local Sherwood number
- t = dimensionless amplitude function of temperature disturbance

- t' = perturbation temperature
- T = fluid temperature
- u, v, w = dimensionless amplitude functions of velocity disturbances
- u', v', w' = axial, normal and spanwise components of velocity disturbances
- U, V = main flow velocity components in x and y directions
- x, y, z = axial, normal and spanwise coordinates
- X, Y, Z = dimensionless streamwise, normal and spanwise coordinate

Greek Symbols

- α = dimensionless wave number of disturbance
- β = $[-(\partial \rho / \partial T)_{p, i}] / \rho$ volumetric coefficient of thermal expansion
- β^* = $[-(\partial \rho / \partial C)_{p, i}] / \rho$ volumetric coefficient of thermal expansion with mass fraction
- δ = boundary layer thickness
- η = Pseudo-similarity variable $(y/r)(Gr_{\lambda T} \cos \phi / 5)^{1/5}$
- η_{δ} = dimensionless boundary layer thickness
- θ = dimensionless temperature $(T - T_{\infty}) / (T_i - T_{\infty})$
- λ = dimensionless mass fraction $(C - C_{\infty}) / (C_{iw}(x) - C_{\infty})$
- κ = thermal diffusivity of fluid
- μ = dynamic viscosity of the fluid
- ν = kinematic viscosity of the fluid
- ξ = $(Gr_{\lambda T} \cos \phi / 5)^{1/5} \tan \phi$ - non-similarity parameter
- ρ = density of fluid
- τ_w = $\mu(\partial u / \partial y)_{y=0} = 0$ local wall shear stress
- ϕ = angle of inclination from the horizontal
- ψ = stream function
- σ = function, $\partial u / \partial \xi$
- ω = function, $\partial v / \partial \xi$
- τ = function, $\partial t / \partial \xi$

Superscripts

- $+$ = dimensionless disturbance quantity
- $-$ = scale quantity
- $*$ = Critical condition or dimensionless main flow quantity
- $=$ Resultant quantity

- = condition at the wall
- = condition at the free stream
- = dimensionless amplitude function

coefficients in eqs (56-63) are given by

$$c_1 = c_2 = c_3 = \alpha^2, a_1 = -5f''(Gr_{1,1} \cos \phi / 5)^{1/5}$$

$$5\xi^2 a_4 = -3f\xi$$

$$\left(f + \xi \frac{\partial f}{\partial \xi} \right), c_2 = (\xi, \eta) = 2\eta f'' - f' - 3\xi^2 \frac{\partial f'}{\partial \xi}$$

$$c_1, b_2 = c_4 = 2\alpha^2, b_1 = 2f'' + \alpha^2 c_1, b_4 = \alpha^4 + \alpha^2 c_2,$$

$$-(c_1 / 5) (Gr_{1,1} \cos \phi / 5)^{1/5}, b_6 = -5\alpha^2 (Gr_{1,1} \cos \phi / 5)^{1/5}$$

$$c_2, b_1 = -3\xi^2 f'', b_9 = 3\alpha^2 \xi f', D^2 \omega = D^2 \left(\frac{\partial \omega}{\partial \xi} \right)$$

$$p_1 = 2\eta f' - 6f + 4\eta^2 f'' + 12\xi \frac{\partial f'}{\partial \xi} - 12\eta \xi \frac{\partial f'}{\partial \xi}$$

$$9\xi^2 \frac{\partial^2 f}{\partial \xi^2}, c_4(\xi, \eta) = 5f' + 3\xi^2 \frac{\partial f'}{\partial \xi}$$

$$d_1 = -Pr c_1, d_2 = -Pr f' - \alpha^2, d_3 = -(Pr/5) c_5,$$

$$d_4 = -Pr \theta (Gr_{1,1} \cos \phi / 5)^{1/5}, d_5 = -3Pr \xi f',$$

$$c_1(\xi, \eta) = 3\xi^2 \frac{\partial \theta}{\partial \xi} - 2\eta \theta'$$

$$c_1 = -Sc c_1, c_2 = -Sc f' - \alpha^2, c_3 = (-Sc/5) c_5,$$

$$c_4 = -Sc \lambda' (Gr_{1,1} \cos \phi / 5)^{1/5}, c_5 = -3Sc \xi f', \frac{\partial c_5}{\partial \xi} = 5$$

$$c_1, f' = c_2 = c_4 + 2f' - \alpha^2, f_1 = -5f''(Gr_{1,1} \cos \phi / 5)^{1/5},$$

$$f_2 = 5\xi, f_3 = 6 \frac{\partial f}{\partial \xi} + 3\xi^2 \frac{\partial^2 f}{\partial \xi^2}$$

$$f_4 = 2\eta \frac{\partial f''}{\partial \xi} - 4 \frac{\partial f'}{\partial \xi} - 3\xi^2 \frac{\partial^2 f''}{\partial \xi^2},$$

$$f_5 = 5(Gr_{1,1} \cos \phi / 5)^{1/5} (c_9 + f'' / \xi), f_8 = 5$$

$$g_1 = -c_1, g_2 = 2f' - 2\alpha^2, g_3 = c_1 \alpha^2 - f'' - 3\xi^2 c_9,$$

$$g_4 = \alpha^4 + \alpha^2 (c_2 + c_4 - 2f'), g_5 = b_1, g_6 = b_6,$$

$$g_7 = c_6, g_8 = c_{10}, g_9 = 2c_9 - \alpha^2 c_6, g_{10} = \alpha^2 c_7,$$

$$g_{11} = \alpha^2 / 5 (Gr_{1,1} \cos \phi / 5)^{1/5} [(c_1 / \xi) - c_8],$$

$$g_{12} = -5\alpha^2 / \xi (Gr_{1,1} \cos \phi / 5)^{1/5}$$

$$c_6(\xi, \eta) = 6 \frac{\partial \theta}{\partial \xi} + 3\xi^2 \frac{\partial^2 \theta}{\partial \xi^2},$$

$$c_7(\xi, \eta) = 2\eta \frac{\partial f''}{\partial \xi} - 4 \frac{\partial f'}{\partial \xi} - 3\xi^2 \frac{\partial^2 f'}{\partial \xi^2},$$

$$c_8(\xi, \eta) = 4\eta^2 \frac{\partial f''}{\partial \xi} - 10\eta \frac{\partial f'}{\partial \xi} + 6 \frac{\partial f}{\partial \xi} + 3\xi^2 \frac{\partial^2 f'}{\partial \xi^2} \xi$$

$$-12\eta \xi \frac{\partial^2 f'}{\partial \xi^2} + 9\xi^2 \frac{\partial^3 f}{\partial \xi^3}$$

$$c_9(\xi, \eta) = \frac{\partial f''}{\partial \xi}, c_{10}(\xi, \eta) = 8 \frac{\partial f'}{\partial \xi} + 3\xi^2 \frac{\partial^2 f'}{\partial \xi^2}$$

$$h_1 = 3Pr \left(f + \xi \frac{\partial f}{\partial \xi} \right), h_2 = -\alpha^2 \left(2f' + 3\xi^2 \frac{\partial f'}{\partial \xi} \right) Pr$$

$$h_3 = -(Pr/5) c_5 = (Pr/5) \left(2\eta \theta' - 3\xi^2 \frac{\partial \theta}{\partial \xi} \right),$$

$$h_4 = -Pr \theta' (Gr_{1,1} \cos \phi / 5)^{1/5}, h_5 = Pr \left(6 \frac{\partial \theta}{\partial \xi} + 3\xi^2 \frac{\partial^2 \theta}{\partial \xi^2} \right),$$

$$h_6 = Pr \frac{\partial f'}{\partial \xi}, h_7 = (-Pr/5) \left(3 \frac{\partial \theta}{\partial \xi} - 2\eta \frac{\partial \theta'}{\partial \xi} + 3\xi^2 \frac{\partial^2 \theta}{\partial \xi^2} \right)$$

$$h_8 = (-Pr/5) (Gr_{1,1} \cos \phi / 5)^{1/5} \left(\theta' + \xi \frac{\partial \theta}{\partial \xi} \right)$$

$$c_{11}(\xi, \eta) = \left(3 \frac{\partial \theta}{\partial \xi} - 2\eta \frac{\partial \theta'}{\partial \xi} + 3\xi^2 \frac{\partial^2 \theta}{\partial \xi^2} \right),$$

$$c_{12}(\xi, \eta) = \theta' + \xi \frac{\partial \theta}{\partial \xi}, c_{13} = \frac{\partial f'}{\partial \xi}$$

$$J_1 = 3Sc \left(f + \xi \frac{\partial f}{\partial \xi} \right), J_2 = -\alpha^2 - \left(2f' + 3\xi^2 \frac{\partial f'}{\partial \xi} - Sc \right)$$

$$J_3 = (-Sc/5) \left(3\xi^2 \frac{\partial \theta}{\partial \xi} - 2\eta \theta' \right),$$

$$J_3 = \left(-Sc/\xi \right) \left(3\xi \frac{\partial \theta}{\partial \xi} - 2\eta \theta' \right),$$

$$J_4 = \left(-Sc/\lambda' \right) \left(Gr_{1,1} \cos \phi / \xi \right)^{1/5}$$

$$J_5 = Sc \left(6 \frac{\partial f}{\partial \xi} + 3\xi \frac{\partial^2 f}{\partial \xi^2} \right), \quad J_6 = Sc \, c_{17},$$

$$J_7 = \left(-Sc/\xi \right) \left(3 \frac{\partial \theta}{\partial \xi} - 2\eta \frac{\partial \theta'}{\partial \xi} + 3\xi \frac{\partial^2 \theta}{\partial \xi^2} \right),$$

$$J_8 = \left(-Sc/\xi \right) \left(Gr_{1,1} \cos \phi / \xi \right)^{1/5} \left(\lambda' + \xi \frac{\partial \lambda'}{\partial \xi} \right),$$

$$\text{and} \quad c_{14}(\xi, \eta) = \lambda' + \xi \frac{\partial \lambda'}{\partial \xi}$$